Payload Estimation Based on Identified Coefficients of Robot Dynamics —with an Application to Collision Detection

Claudio Gaz   Alessandro De Luca

Abstract— We revisit the classical problem of estimating the dynamic parameters of an unknown payload rigidly held by the robot end effector. The approach relies on the analysis of the symbolic expressions of the robot dynamic coefficients (i.e., combinations of dynamic parameters) when working with and without payload, with no special assumptions on payload structure. The linearity of the associated changes in the dynamic coefficients due to the payload addition is exploited so as to estimate the gravity and inertial parameters of the payload. The procedure is illustrated in simulation on a planar 2R robot with asymmetric payload and through experiments on a 7R KUKA LWR arm with medium payloads. Accurate estimates of non-inertial payload parameters can be obtained even by running the identification scheme on few small motions in a restricted area. The results are shown to be useful for improving the sensorless collision detection capabilities of a robot arm in the presence of an a priori unknown payload.

I. INTRODUCTION

Complete and accurate dynamic models of robot manipulators are needed in the design of advanced control laws, both for free motion and in environment interaction [1]. In addition, recent methods for safe handling of human-robot interaction rely on a good knowledge of the individual terms in the robot dynamic model, e.g., for designing a sensorless strategy to detect and react to collisions [2], or for regulating force or imposing a desired impedance at the contact [3], [4].

For control purposes, it is often sufficient to identify the so-called *dynamic coefficients*, also known as base parameters, in the robot equations of motions [5], [6]. These coefficients are combinations of the *dynamic parameters* of the (serial) chain of bodies constituting the robot — 10 parameters for each link (the scalar mass, the three components of the position vector of the center of mass, and the six elements of the symmetric inertia tensor), plus additional parameters local to each joint, when including in the model also friction effects, motor inertias, current-to-torque ratios, transmission elasticity, and so on. The dynamic coefficients always appear linearly in the second-order differential equations of the robot. They represent the dynamic quantities that can be excited during motion and thus properly identified —see [5], [7] for state-of-the-art identification methods and [8], [9] for variants in case of the KUKA LWR robot equipped with joint torque sensors.

On the other hand, there is no guarantee of identifiability of all dynamic parameters for a multi-body robot. Nonethe-

less, numerical values of the dynamic parameters of the robot links are needed in some applications, for example when performing dynamic simulations with standard CAD-based systems like V-REP [10], or when the use of an efficient recursive Newton-Euler (N-E) algorithm [11] is mandatory for implementing complex model-based control laws (e.g., feedback linearization) under hard real-time constraints. In such cases, wishing to avoid an additional customization, all dynamic parameters (and not just the dynamic coefficients) will be required as input data. To address this issue, we proposed in [12] a handy method for extracting from the previously identified robot dynamic coefficients a complete set of *feasible* dynamic parameters, which are consistent with (i.e., return back) the numerical values of the coefficients and satisfy also physical, user-defined upper and lower bounds.

In this paper we consider the problem of estimating the 10 extra dynamic parameters of an unknown payload rigidly held by the end effector of a robot, without resorting to extra sensory systems (e.g., a F/T sensor as in [13]). This is a classical topic for which model-based strategies [14], [15] or machine learning techniques using neural networks [16], [17] have been proposed. Model-based methods consider two sets of experiments made first without and then with the payload. Here, we revisit and clarify an identification scheme that can use either the previously estimated dynamic coefficients of the robot without payload or the values of feasible dynamic parameters extracted from them. The structural changes due to the presence of a payload occurring in the symbolic form of the dynamic coefficients of the loaded robot are exploited in order to set up the regressor equations for payload identification. In this framework, we address in particular the following questions:

Q1. What is the rule of change of the original dynamic coefficients when a payload is added?

Q2. Do we obtain again a linearly parametrized problem? And does this property rely on some specific choice of reference frames, e.g., the conventional [1] or the modified [15] Denavit-Hartenberg (DH) assignments, or any convention can be used?

Q3. Can we estimate the entire set of 10 dynamic parameters of the payload from the values of the robot dynamic coefficients identified with and without the payload?

Q4. Can we use the estimated parameters of the payload in combination with any set of feasible dynamic parameters for the unloaded robot (for instance, in a NE-based control routine), obtaining consistently good results?

We will provide constructive answers to these questions.

After reviewing the basics of modeling and identification procedures (Sec. II), Section III provides a closed-form expression of the changes in the robot dynamic coefficients when a payload is added, and sets up the payload identification procedure. Two illustrative case studies are considered: estimation of an asymmetric payload for a planar 2R robot, with validation results obtained in simulation (Sec. IV), and experimental estimation of all dynamic parameters of both a heavy and a very light payload carried by a KUKA LWR 4+ robot (Sec. V). Finally, in Sec. VI further experimental results are presented when running the identification scheme on few small motions in a restricted area, and when using the obtained payload estimate to improve the robot collision detection capabilities.

II. PRELIMINARIES

For each link ℓ_i, $i = 1, \ldots, n$, of a n-dof robot, let m_i be the mass and

$$
{}^i\boldsymbol{r}_{i,ci} = \begin{pmatrix} c_{ix} \\ c_{iy} \\ c_{iz} \end{pmatrix}^T, \quad {}^i\boldsymbol{I}_{\ell_i} = \begin{pmatrix} I_{ixx} & I_{ixy} & I_{ixz} \\ I_{ixy} & I_{iyy} & I_{iyz} \\ I_{ixz} & I_{iyz} & I_{izz} \end{pmatrix}, \quad (1)
$$

be respectively the position of the center of mass (CoM) with respect to the i-th link frame and the symmetric inertia tensor relative to the CoM of link i (both constant).

With $\boldsymbol{q} \in \mathbb{R}^n$ as generalized coordinates, the total potential energy $\mathcal{U} = \mathcal{U}(\boldsymbol{q})$ of the robot is

$$
\mathcal{U} = \sum_{i=1}^n \mathcal{U}_{\ell_i} = -\sum_{i=1}^n m_i \boldsymbol{\gamma}^T \boldsymbol{r}_{0,ci}, \qquad (2)
$$

where $\boldsymbol{\gamma}(g_0)$ is the gravity vector in the absolute reference frame and $g_0 = 9.81$ the gravity acceleration. By using homogeneous transformation matrices, the absolute position $\boldsymbol{r}_{0,ci}$ of the center of mass of link i is obtained from ${}^i\boldsymbol{r}_{i,ci}$ and will depend linearly on it.

The total kinetic energy $\mathcal{T} = \mathcal{T}(\boldsymbol{q}, \dot{\boldsymbol{q}})$ uses König theorem for each link,

$$
\mathcal{T} = \sum_{i=1}^n \mathcal{T}_{\ell_i} = \frac{1}{2} \sum_{i=1}^n \left(m_i {}^i\boldsymbol{v}_{ci}^T {}^i\boldsymbol{v}_{ci} + {}^i\boldsymbol{\omega}_i^T {}^i\boldsymbol{I}_{\ell_i} {}^i\boldsymbol{\omega}_i \right), \quad (3)
$$

in which ${}^i\boldsymbol{v}_{ci}$ is the linear velocity of the CoM of link i and ${}^i\boldsymbol{\omega}_i$ is the angular velocity of the link i, both expressed in the local frame. The velocity ${}^i\boldsymbol{v}_{ci}$ can be related to the linear velocity ${}^i\boldsymbol{v}_i$ of the origin of a known, generic kinematic frame i as

$$
{}^i\boldsymbol{v}_{ci} = {}^i\boldsymbol{v}_i + \boldsymbol{S}\left({}^i\boldsymbol{\omega}_i\right){}^i\boldsymbol{r}_{i,ci} = {}^i\boldsymbol{v}_i + \boldsymbol{S}^T\left({}^i\boldsymbol{r}_{i,ci}\right){}^i\boldsymbol{\omega}_i, \quad (4)
$$

where $\boldsymbol{S}(\cdot)$ is the skew-symmetric operator representing the vector ($\times$) product. Moreover, the inertia tensor ${}^i\boldsymbol{I}_{\ell_i}$ is expressed with respect to the same local frame i as

$$
{}^i\boldsymbol{J}_{\ell_i} = \begin{pmatrix} J_{ixx} & J_{ixy} & J_{ixz} \\ J_{ixy} & J_{iyy} & J_{iyz} \\ J_{ixz} & J_{iyz} & J_{izz} \end{pmatrix} = {}^i\boldsymbol{I}_{\ell_i} + m_i \boldsymbol{S}^T\left({}^i\boldsymbol{r}_{i,ci}\right)\boldsymbol{S}\left({}^i\boldsymbol{r}_{i,ci}\right).
$$
(5)

Therefore, we can rewrite eq. (3) as

$$
\mathcal{T} = \frac{1}{2} \sum_{i=1}^n \left(m_i \|{}^i\boldsymbol{v}_i\|^2 + {}^i\boldsymbol{\omega}_i^T {}^i\boldsymbol{J}_{\ell_i} {}^i\boldsymbol{\omega}_i + 2m_i {}^i\boldsymbol{r}_{i,ci}^T \left({}^i\boldsymbol{v}_i \times {}^i\boldsymbol{\omega}_i\right) \right).
$$
(6)

From the Euler-Lagrange equations, we obtain the robot dynamic model as

$$
\boldsymbol{M}(\boldsymbol{q})\ddot{\boldsymbol{q}} + \boldsymbol{S}(\boldsymbol{q}, \dot{\boldsymbol{q}})\dot{\boldsymbol{q}} + \boldsymbol{g}(\boldsymbol{q}) = \boldsymbol{\tau}, \qquad (7)
$$

where the inertia matrix and the gravity vector follow from symbolic differentiation of the kinetic energy $\mathcal{T}$ and potential energy $\mathcal{U}$ as

$$
\boldsymbol{M}(\boldsymbol{q}) = \nabla_{\dot{\boldsymbol{q}}}^2 \mathcal{T}(\boldsymbol{q}, \dot{\boldsymbol{q}}) \in \mathbb{R}^{n \times n}, \quad \boldsymbol{g}(\boldsymbol{q}) = \nabla_{\boldsymbol{q}} \mathcal{U}(\boldsymbol{q}) \in \mathbb{R}^n, \quad (8)
$$

the Coriolis and centrifugal term $\boldsymbol{S}(\boldsymbol{q}, \dot{\boldsymbol{q}})\dot{\boldsymbol{q}} \in \mathbb{R}^n$ is obtained by analytic differentiation of the elements of $\boldsymbol{M}(\boldsymbol{q})$ [1], and $\boldsymbol{\tau} \in \mathbb{R}^n$ is the vector of motor torques.

At this stage, if we use the form (6) for the kinetic energy and collect the dynamic parameters of all the robot links in the three vectors $\boldsymbol{p}_1 \in \mathbb{R}^n$, $\boldsymbol{p}_2 \in \mathbb{R}^{3n}$, and $\boldsymbol{p}_3 \in \mathbb{R}^{6n}$, with

$$
\boldsymbol{p}_1 = \begin{pmatrix} m_1 & \ldots & m_n \end{pmatrix}^T,
$$
$$
\boldsymbol{p}_2 = \begin{pmatrix} c_{1x}m_1 & c_{1y}m_1 & c_{1z}m_1 & \ldots & c_{nx}m_n & c_{ny}m_n & c_{nz}m_n \end{pmatrix}^T,
$$
$$
\boldsymbol{p}_3 = \begin{pmatrix} \mathcal{J}_1^T & \ldots & \mathcal{J}_n^T \end{pmatrix}^T,
$$
(9)

where

$$
\mathcal{J}_i = \begin{pmatrix} J_{ixx} & J_{ixy} & J_{ixz} & J_{iyy} & J_{iyz} & J_{izz} \end{pmatrix}^T, \quad (10)
$$

then it is possible to rearrange (7) as

$$
\boldsymbol{Y}(\boldsymbol{q}, \dot{\boldsymbol{q}}, \ddot{\boldsymbol{q}})\boldsymbol{\pi}(\boldsymbol{p}_1, \boldsymbol{p}_2, \boldsymbol{p}_3) = \boldsymbol{\tau}. \qquad (11)
$$

The vector $\boldsymbol{\pi} \in \mathbb{R}^p$ of dynamic coefficients appears linearly in the dynamic model (11), multiplied by the $n \times p$ regressor matrix $\boldsymbol{Y}$ of known time-varying functions. Moreover, it can be easily shown that only linear combinations of the dynamic parameters in (9) will appear in the dynamic coefficients $\boldsymbol{\pi}$.

When the regressor $\boldsymbol{Y}$ has full rank, the dynamic coefficients $\boldsymbol{\pi}$ are identified by collecting $M \gg np$ motor torque samples (as obtained from the commanded motor currents) as well as M link position samples from a sufficiently exciting motion, while velocity and acceleration are computed by off-line differentiation. For each retrieved numerical sample $(\boldsymbol{\tau}_k, \boldsymbol{q}_k, \dot{\boldsymbol{q}}_k, \ddot{\boldsymbol{q}}_k)$, we have

$$
\boldsymbol{Y}_k(\boldsymbol{q}_k, \dot{\boldsymbol{q}}_k, \ddot{\boldsymbol{q}}_k)\boldsymbol{\pi} = \boldsymbol{\tau}_k, \qquad k = 1, \ldots, M. \quad (12)
$$

By stacking these quantities in vectors and matrices, one has

$$
\overline{\boldsymbol{Y}}\boldsymbol{\pi} = \overline{\boldsymbol{\tau}}, \qquad (13)
$$

with $\overline{\boldsymbol{\tau}} \in \mathbb{R}^{Mn}$ and $\overline{\boldsymbol{Y}} \in \mathbb{R}^{Mn \times p}$. Following [8], we can prune the stacked regressor $\overline{\boldsymbol{Y}}$ so as to obtain a matrix with full column rank, and then estimate the dynamic coefficients by solving a least-squares problem via pseudoinversion

$$
\hat{\boldsymbol{\pi}} = \overline{\boldsymbol{Y}}^{\#}\overline{\boldsymbol{\tau}}. \qquad (14)
$$

With the solution $\hat{\boldsymbol{\pi}}$ from (14), we provide an associated motor torque estimate as

$$\hat{\boldsymbol{\tau}} = \boldsymbol{Y}(\boldsymbol{q}, \dot{\boldsymbol{q}}, \ddot{\boldsymbol{q}})\hat{\boldsymbol{\pi}} \tag{15}$$

which can be used for validation on any new robot motion $\boldsymbol{q}(t)$. Finally, following [12], one can extract from the identified vector $\hat{\boldsymbol{\pi}}$ a feasible set of dynamic parameters $\hat{\boldsymbol{p}} = (\hat{\boldsymbol{p}}_1, \hat{\boldsymbol{p}}_2, \hat{\boldsymbol{p}}_3)$ —not necessarily the true ones—, such that $\boldsymbol{\pi}(\hat{\boldsymbol{p}}_1, \hat{\boldsymbol{p}}_2, \hat{\boldsymbol{p}}_3) = \hat{\boldsymbol{\pi}}$ and upper/lower bounds on the components of $\boldsymbol{p}_i$, $i = 1, 2, 3$, are also satisfied.

III. MODIFIED DYNAMIC COEFFICIENTS DUE TO A PAYLOAD

We assume that accurate values of the robot dynamic coefficients have been identified in the absence of a payload. An unknown rigid payload is then added on the robot end effector, having mass m_L, position of its CoM with respect to the last frame n given by ${}^n\boldsymbol{r}_{n,cL} = \begin{pmatrix} c_{Lx} & c_{Ly} & c_{Lz} \end{pmatrix}^T$, and a 3×3 inertia tensor $\boldsymbol{J}_L$ relative to the last frame n. Under these assumptions, the dynamic parameters of the last robot link n will change as

$$
\begin{aligned}
& c_{nx} \;\rightarrow\; \frac{c_{nx}m_n + c_{Lx}m_L}{m_n + m_L} \\
m_n \rightarrow m_n + m_L, \quad & c_{ny} \;\rightarrow\; \frac{c_{ny}m_n + c_{Ly}m_L}{m_n + m_L} \\
& c_{nz} \;\rightarrow\; \frac{c_{nz}m_n + c_{Lz}m_L}{m_n + m_L},
\end{aligned}
\tag{16}
$$

$$
\boldsymbol{J}_n \rightarrow \boldsymbol{J}_n + \boldsymbol{J}_L =
$$
$$
\begin{pmatrix}
J_{nxx} + J_{Lxx} & J_{nxy} + J_{Lxy} & J_{nxz} + J_{Lxz} \\
J_{nxy} + J_{Lxy} & J_{nyy} + J_{Lyy} & J_{nyz} + J_{Lyz} \\
J_{nxz} + J_{Lxz} & J_{nyz} + J_{Lyz} & J_{nzz} + J_{Lzz}
\end{pmatrix}. \tag{17}
$$

Note that weighted averages appear in (16). Moreover, addition of the two inertia tensors of the last link and payload in (17) is feasible, being both expressed in the same kinematic frame. If the inertia tensor $\boldsymbol{I}_L$ of the payload were expressed instead in a frame placed in the payload CoM that is not oriented as frame n, we define the rotation matrix ${}^n\boldsymbol{R}_L$ and then use Steiner theorem to obtain

$$\boldsymbol{J}_L = {}^n\boldsymbol{R}_L\,\boldsymbol{I}_L\,{}^n\boldsymbol{R}_L^T + m_L\,\boldsymbol{S}^T\left({}^n\boldsymbol{r}_{n,cL}\right)\boldsymbol{S}\left({}^n\boldsymbol{r}_{n,cL}\right). \tag{18}$$

In the parametrization (9), the coordinates of the CoM of a link always appear multiplied by the mass of the link they refer to. Most notably, when modifying the dynamic parameters of the last link as in (16), we will obtain

$$
\begin{aligned}
c_{nx}m_n &\;\rightarrow\; \tfrac{c_{nx}m_n + c_{Lx}m_L}{m_n + m_L}(m_n + m_L) = c_{nx}m_n + c_{Lx}m_L \\
c_{ny}m_n &\;\rightarrow\; \tfrac{c_{ny}m_n + c_{Ly}m_L}{m_n + m_L}(m_n + m_L) = c_{ny}m_n + c_{Ly}m_L \\
c_{nz}m_n &\;\rightarrow\; \tfrac{c_{nz}m_n + c_{Lz}m_L}{m_n + m_L}(m_n + m_L) = c_{ny}m_n + c_{Ly}m_L,
\end{aligned}
\tag{19}
$$

preserving the linearity of the parameter transformation.

A. Estimating the dynamic parameters of the payload

Let the vector $\boldsymbol{p}_L$ of dynamic parameters of the payload be defined as

$$\boldsymbol{p}_L = \begin{pmatrix} m_L & c_{Lx}m_L & c_{Ly}m_L & c_{Lz}m_L & \mathcal{J}_L \end{pmatrix}^T \in \mathbb{R}^{10}. \tag{20}$$

We consider two different vectors of dynamic coefficients, labeled $\boldsymbol{\pi} = \boldsymbol{\pi}(\boldsymbol{p}_1, \boldsymbol{p}_2, \boldsymbol{p}_3)$ and $\boldsymbol{\pi}_L = \boldsymbol{\pi}_L(\boldsymbol{p}_1, \boldsymbol{p}_2, \boldsymbol{p}_3, \boldsymbol{p}_L)$, respectively in the absence and presence of the payload. The *symbolic* difference vector

$$\boldsymbol{\varepsilon}(\boldsymbol{p}_L) = \boldsymbol{\pi}_L(\boldsymbol{p}_1, \boldsymbol{p}_2, \boldsymbol{p}_3, \boldsymbol{p}_L) - \boldsymbol{\pi}(\boldsymbol{p}_1, \boldsymbol{p}_2, \boldsymbol{p}_3) \tag{21}$$

contains indeed combinations of the dynamic parameters of the payload. Equations (16–17), (19), and (21) answer to the introductory question Q1. Note that some components of $\boldsymbol{\varepsilon}$ will vanish, namely those that are not affected by the addition of the payload. We shall discard these zero components and label the remaining vector as $\boldsymbol{\varepsilon}_{nz}$.

Assume that a reliable estimate $\hat{\boldsymbol{\pi}}$ of $\boldsymbol{\pi}$ has been obtained in advance (without the payload). When the unknown payload is present, thanks to (21), we can write for the dynamics of the loaded robot

$$\boldsymbol{Y}_L(\boldsymbol{q}, \dot{\boldsymbol{q}}, \ddot{\boldsymbol{q}})\boldsymbol{\pi}(\boldsymbol{p}_1, \boldsymbol{p}_2, \boldsymbol{p}_3) + \boldsymbol{Y}_L(\boldsymbol{q}, \dot{\boldsymbol{q}}, \ddot{\boldsymbol{q}})\boldsymbol{\varepsilon}(\boldsymbol{p}_L) = \boldsymbol{\tau}_L, \tag{22}$$

where $\boldsymbol{Y}_L$ is the same regressor matrix of the unloaded case, evaluated under the action of the torque $\boldsymbol{\tau}_L$ and in the presence of the payload. Equation (22) reveals a superposition property when adding a payload, given the linearity in the dynamic coefficients. Thus, the estimated dynamic behavior of the loaded robot will be the same no matter if the estimated dynamic coefficients $\hat{\boldsymbol{\pi}}$ or some feasible set of estimated values $\hat{\boldsymbol{p}}$ for the parameters are used.

The identification procedure for the payload parameters $\boldsymbol{p}_L$ works similarly to the unloaded case, but takes advantage of the previously estimated dynamic coefficients $\hat{\boldsymbol{\pi}}$. The robot will execute a set of sufficiently exciting trajectories [18], which may be the same or differ from those of the unloaded case. We collect motor torques $\overline{\boldsymbol{\tau}}_L$ and motion data, process them and organize a linear set of equations as

$$\overline{\boldsymbol{Y}}_L\boldsymbol{\pi}_L = \overline{\boldsymbol{\tau}}_L, \tag{23}$$

where $\overline{\boldsymbol{Y}}_L$ is the stacked regressor evaluated during the set of experiments. The estimated coefficients of the loaded case are again computed as

$$\hat{\boldsymbol{\pi}}_L = \overline{\boldsymbol{Y}}_L^{\#}\overline{\boldsymbol{\tau}}_L, \tag{24}$$

and, using (14), we obtain the *numerical* difference vector $\hat{\boldsymbol{\varepsilon}}$ as

$$\hat{\boldsymbol{\varepsilon}} = \hat{\boldsymbol{\pi}}_L - \hat{\boldsymbol{\pi}}. \tag{25}$$

We note that in some cases, the robot control software (e.g., the KUKA FRI interface) provides the user with numerical values of the joint torques associated to a static configuration or to the dynamic trajectory under execution, computed without consideration of the presence or not of a payload. Let $\overline{\boldsymbol{\tau}}$ be the stacked vector of these torques with the robot

carrying the unknown payload. We can compute then the estimate as

$$\hat{\varepsilon} = \overline{\boldsymbol{Y}}_L^{\#}\,\overline{\Delta\boldsymbol{\tau}}, \qquad \text{with } \overline{\Delta\boldsymbol{\tau}} = \overline{\boldsymbol{\tau}}_L - \overline{\boldsymbol{\tau}}, \qquad (26)$$

where $\overline{\boldsymbol{\tau}}_L$ is the stacked torque measured during the loaded experiment. Hence, in this case there is no need to estimate the vectors $\hat{\boldsymbol{\pi}}$ and $\hat{\boldsymbol{\pi}}_L$, nor of using data from experiments without the payload. A one-shot solution is obtained.

Independently from the use of eq. (25) or (26), by defining the *payload Jacobian* $\boldsymbol{J}_\varepsilon$ as the matrix of symbolic partial derivatives of $\varepsilon(\boldsymbol{p}_L)$ with respect to vector $\boldsymbol{p}_L$, we have

$$\boldsymbol{J}_\varepsilon = \frac{\partial\varepsilon(\boldsymbol{p}_L)}{\partial\boldsymbol{p}_L} \quad \Rightarrow \quad \boldsymbol{J}_\varepsilon\boldsymbol{p}_L = \varepsilon. \qquad (27)$$

Equation (27) gives a positive answer to question Q2. Moreover, in view of the analysis in Sec. II, this result holds whatever kinematic frame convention is adopted. Therefore, the payload parameters are estimated as

$$\hat{\boldsymbol{p}}_L = \boldsymbol{J}_\varepsilon^{\#}\hat{\varepsilon}. \qquad (28)$$

Note also that it is convenient to reduce the Jacobian evaluation only to the non-zero components $\varepsilon_{nz}(\boldsymbol{p}_L)$ of ε. Having obtained the estimate $\hat{m}_L$ in $\hat{\boldsymbol{p}}_L$, it is immediate to isolate $\hat{c}_{Lx}$, $\hat{c}_{Ly}$, and $\hat{c}_{Lz}$ from the estimated $\widehat{c_{Lx}m_L}$, $\widehat{c_{Ly}m_L}$, and $\widehat{c_{Lz}m_L}$. The inertial elements of the payload are instead estimated directly. Thus, the answer to question Q3 is again yes, provided that the regressors and the payload Jacobian will have full rank.

IV. Payload estimation in a 2R planar robot

We illustrate the procedure first on a 2R planar robot moving under gravity with $\boldsymbol{\gamma} = \begin{pmatrix} 0 & -g_0 \end{pmatrix}^T$, with or without an *asymmetric* payload, see Fig. 1. Because of the planar nature of the problem, only four parameters for each link and for the payload will influence the robot dynamics — in total 12 dynamic parameters: the three masses m_1, m_2, and m_L, the three positions of the CoMs in the plane, respectively, $\boldsymbol{r}_{1,c1} = \begin{pmatrix} c_{1x} & c_{1y} \end{pmatrix}^T$, $\boldsymbol{r}_{2,c2} = \begin{pmatrix} c_{2x} & c_{2y} \end{pmatrix}^T$, and $\boldsymbol{r}_{2,cL} = \begin{pmatrix} c_{Lx} & c_{Ly} \end{pmatrix}^T$, and the scalar elements J_{1zz}, J_{2zz}, and J_{Lzz} of the inertia tensors.

Deriving the dynamic model (7) and rearranging it as in (11), we obtain the vector of dynamic coefficients $\boldsymbol{\pi} \in \mathbb{R}^6$

$$\boldsymbol{\pi} = \begin{pmatrix} \frac{1}{2}\left(m_2 a_2^2 + J_{2zz}\right) + a_2 c_{2x} m_2 \\ c_{2x} m_2 + a_2 m_2 \\ c_{2y} m_2 \\ \frac{1}{2}\left(J_{1zz} + a_1^2 m_1 + a_1^2 m_2\right) + a_1 c_{1x} m_1 \\ c_{1x} m_1 + a_1 m_1 + a_1 m_2 \\ c_{1y} m_1 \end{pmatrix}, \qquad (29)$$

where a_1 and a_2 are known kinematic parameters. We have chosen the following kinematic and nominal dynamic values: $a_1 = 1$, $a_2 = 0.5$ [m]; $m_1 = 3$, $m_2 = 2$ [kg]; $c_{1x} = -0.6$, $c_{1y} = 0.01$, $c_{2x} = -0.2$, $c_{2y} = 0.02$ [m]; $J_{1zz} = 1.3303$, $J_{2zz} = 0.1225$ [kg·m^2].
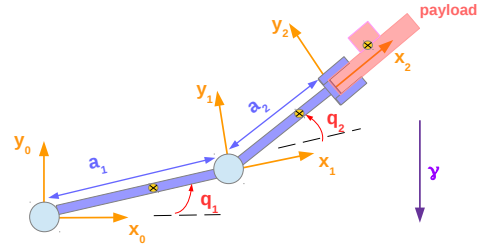

Fig. 1. A 2R planar robot carrying an asymmetrical payload, with the chosen conventional Denavit-Hartenberg frames.

When a payload is added, the new vector of dynamic coefficients $\boldsymbol{\pi}_L \in \mathbb{R}^6$ becomes

$$\boldsymbol{\pi}_L = \begin{pmatrix} \frac{1}{2}\left(a_2^2(m_2+m_L)+J_{2zz}+J_{Lzz}\right) + a_2\left(c_{2x}m_2+c_{Lx}m_L\right) \\ c_{2x}m_2 + c_{Lx}m_L + a_2\left(m_2 + m_L\right) \\ c_{2y}m_2 + c_{Ly}m_L \\ \frac{1}{2}\left(J_{1zz} + a_1^2 m_1 + a_1^2(m_2 + m_L)\right) + a_1 c_{1x} m_1 \\ c_{1x}m_1 + a_1 m_1 + a_1\left(m_2 + m_L\right) \\ c_{1y}m_1 \end{pmatrix}. \qquad (30)$$

The values of the payload parameters considered as ground truth are: $m_L = 1.5$ [kg]; $c_{Lx} = 0.3$, $c_{Ly} = 0.1$ [m]; and $J_{Lzz} = 0.1813$ [kg·m^2].

The symbolic expression of $\varepsilon(\boldsymbol{p}_L)$ in (21) is

$$\varepsilon(\boldsymbol{p}_L) = \begin{pmatrix} \varepsilon_{nz}(\boldsymbol{p}_L) \\ 0 \end{pmatrix} = \begin{pmatrix} \frac{1}{2}\left(a_2^2 m_L + J_{Lzz}\right) + a_2 c_{Lx} m_L \\ c_{Lx}m_L + a_2 m_L \\ c_{Ly}m_L \\ \frac{1}{2}a_1^2 m_L \\ a_1 m_L \\ 0 \end{pmatrix}. \qquad (31)$$

The Jacobian in (27) is evaluated in its reduced form as

$$\boldsymbol{J}_{\varepsilon,nz} = \frac{\partial\varepsilon_{nz}(\boldsymbol{p}_L)}{\partial\boldsymbol{p}_L} = \begin{pmatrix} \frac{1}{2}a_2^2 & a_2 & 0 & \frac{1}{2} \\ a_2 & 1 & 0 & 0 \\ 0 & 0 & 1 & 0 \\ \frac{1}{2}a_1^2 & 0 & 0 & 0 \\ a_1 & 0 & 0 & 0 \end{pmatrix}, \qquad (32)$$

being

$$\boldsymbol{p}_L = \begin{pmatrix} m_L & c_{Lx}m_L & c_{Ly}m_L & J_{Lzz} \end{pmatrix}^T. \qquad (33)$$

Two sets of joint torques have been generated in a slightly noisy simulation, with the robot tracking two sinusoidal reference trajectories of different amplitude and frequency for each joint. The values were collected as stacks $\overline{\boldsymbol{\tau}}$ (without payload) and $\overline{\boldsymbol{\tau}}_L$ (with payload). Using eqs. (14) and (24), the estimates $\hat{\boldsymbol{\pi}}$ and $\hat{\boldsymbol{\pi}}_L$, and from these the numerical vector $\hat{\varepsilon}_{nz}$, are obtained as

$$\hat{\boldsymbol{\pi}} = \begin{pmatrix} 0.1112 \\ 0.6 \\ 0.04 \\ 1.3651 \\ 3.2 \\ 0.03 \end{pmatrix}, \; \hat{\boldsymbol{\pi}}_L = \begin{pmatrix} 0.6144 \\ 1.8 \\ 0.19 \\ 2.1152 \\ 4.7 \\ 0.03 \end{pmatrix} \Rightarrow \hat{\varepsilon}_{nz} = \begin{pmatrix} 0.5032 \\ 1.2 \\ 0.15 \\ 0.75 \\ 1.5 \end{pmatrix}. \qquad (34)$$
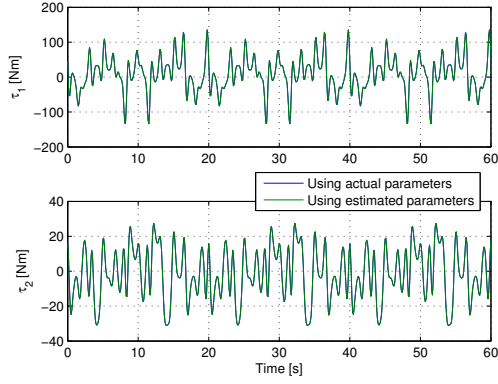
Fig. 2. Comparison of torques in a validation test on the 2R robot using the true [blue] and the estimated [green] dynamic parameters. The plots fully superpose in practice: the mean square error is 3.187 $[Nm]^2$ for τ_1 and 0.387 $[Nm]^2$ for τ_2.

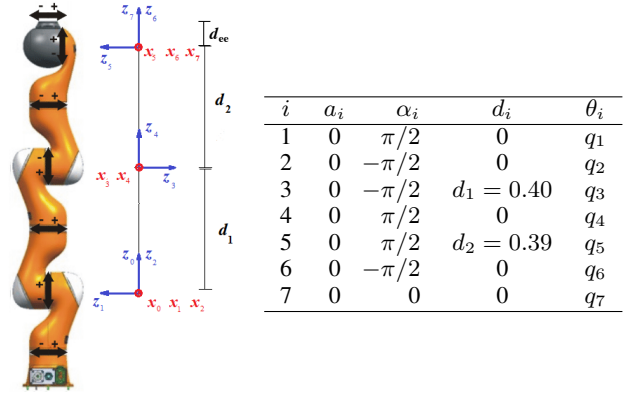

Fig. 3. Denavit-Hartenberg frames and parameters of the KUKA LWR 4+. All x-axes point toward the viewer (frames displaced sideways for clarity).

Using (28) and the payload Jacobian in (32) yields the following estimate for p_L in (33):

$$\hat{p}_L = \begin{pmatrix} 1.5 & 0.45 & 0.15 & 0.1814 \end{pmatrix}^T. \quad (35)$$

Being $\hat{m}_L = 1.5$, from the second and third components we obtain $\hat{c}_{Lx} = 0.3$ and $\hat{c}_{Ly} = 0.1$. Thus, the obtained estimates match perfectly the ground truth.

As a final validation, following the procedure in [12], we searched for a feasible set of dynamic parameters extracted from $\hat{\pi}$ in (34), namely for the robot without payload, and belonging to the interval defined by lower and upper bounds on the 8 relevant dynamic parameters of the two links (in the order m_1, m_2, J_{1zz}, J_{2zz}, c_{1x}, c_{1y}, c_{2x}, c_{2y})

$$LB = \begin{pmatrix} 0 & 0 & 0 & 0 & -1 & -0.02 & -0.5 & -0.02 \end{pmatrix}^T$$
$$UB = \begin{pmatrix} 5 & 3 & 2 & 1 & 0 & 0.02 & 0 & 0.02 \end{pmatrix}^T, \quad (36)$$

with the additional global constraint $3 \leq m_1 + m_2 \leq 6$. The optimization problem defined in [12] returns the solution:

$$\hat{p} = \big(1.5064 \quad 2.4598 \quad 0.2965 \quad 0.2374$$
$$-0.5086 \quad 0.0199 \quad -0.2561 \quad 0.0163\big)^T. \quad (37)$$

Next, the payload was added and the parameters $\hat{m}_2$, $\hat{c}_{2x}$, $\hat{c}_{2y}$, and $\hat{J}_{2zz}$ of link 2 in (37) were modified according to (16–17) and (19), with the payload estimates in (35). To address in practice question Q4, a N-E routine was fed with all these data in order to compute the inverse dynamics torque needed to execute sinusoidal motions for both joints (with amplitude 2π rad and frequency 0.05 Hz for joint 1, and π rad and 0.3 Hz for joint 2). Figure 2 compares the torques obtained using the true and the estimated dynamic parameters. As expected, the two plots are overlapping.

V. PAYLOAD ESTIMATION IN A KUKA LWR 4+ ROBOT

We applied the proposed identification procedure to a KUKA LWR 4+ robot. In the experiments, we have used the embedded joint torque sensors to measure the (elastic) joint torques τ_J in place of the motor torques τ. In this case, the left-hand sides of (7) and (11) represent the dynamics of

the robot links (beyond the elasticity at the joints). Figure 3 shows this 7R robot arm in the $q = 0$ position, together with the link frames and the table of kinematic parameters chosen according to the classical DH convention.

In [8], we have identified the dynamic coefficients of the gravity vector and of the inertia matrix that are used by the KRC (Kuka Robot Controller) in FRI mode to return online the numerical values of these model terms [19], [20]. In particular, we reported the symbolic form of the 12 dynamic coefficients π_g appearing in the gravity vector (see eq. (28) in [8]). When incorporating a payload on the end effector, these coefficients will be modified according to (16) as

$$\pi_{L,g} = \begin{pmatrix} c_{7y}m_7 + c_{Ly}m_L \\ c_{7x}m_7 + c_{Lx}m_L \\ c_{6x}m_6 \\ c_{6z}m_6 + c_{7z}m_7 + c_{Lz}m_L \\ c_{5z}m_5 - c_{6y}m_6 \\ c_{5x}m_5 \\ c_{5y}m_5 + c_{4z}m_4 + d_2(m_5 + m_6 + m_7 + m_L) \\ c_{4x}m_4 \\ c_{4y}m_4 + c_{3z}m_3 \\ c_{2x}m_2 \\ c_{3x}m_3 \\ c_{2z}m_2 - c_{3y}m_3 \\ + d_1(m_3 + m_4 + m_5 + m_6 + m_7 + m_L) \end{pmatrix}, \quad (38)$$

where m_L is the mass and $^7r_{7,cL} = \begin{pmatrix} c_{Lx} & c_{Ly} & c_{Lz} \end{pmatrix}^T$ is the payload CoM position, expressed in the robot frame 7.

The composite payload that we used is shown in Fig. 4. Since the structure of the payload is always symmetric, we set $c_{Lx} = c_{Ly} = 0$, while we computed the value of c_{Lz} from (simplified) geometry. The results reported here refer to the nominal values:

$$m_L = 3.028 \text{ kg}, \qquad ^7r_{7,cL} = \begin{pmatrix} 0 \\ 0 \\ 0.1190 \end{pmatrix} \text{ m}. \quad (39)$$

Using (38), it is possible to estimate first and separately the non-inertial dynamic parameters $p_{L,g}$ of the payload, i.e., those excited by gravity:

$$p_{L,g} = \begin{pmatrix} m_L & c_{Lx}m_L & c_{Ly}m_L & c_{Lz}m_L \end{pmatrix}^T \in \mathbb{R}^4. \quad (40)$$

For this, 500 random joint configurations were chosen, the robot was moved to each configuration in sequence and then kept still, and the measured joint torques $\boldsymbol{\tau}_J$ were retrieved in static conditions using the FRI function `GetMeasuredJointTorques`. Since $\dot{\boldsymbol{q}} = \ddot{\boldsymbol{q}} = \mathbf{0}$, we have from (7) and (11)

$$\boldsymbol{g}(\boldsymbol{q}) = \boldsymbol{Y}_g(\boldsymbol{q})\boldsymbol{\pi}_g, \qquad \boldsymbol{Y}_g(\boldsymbol{q})\boldsymbol{\pi}_g + \boldsymbol{\nu} = \boldsymbol{\tau}_J, \qquad (41)$$

where $\boldsymbol{\nu}$ represents noise due to some unmodeled effects. Following the identification procedure, we collected stacks of joint torque measurements and of joint positions, respectively without and with payload. We discarded then the data from joint 1, since this joint is not affected by gravity. The obtained numerical estimates are:

$$\hat{\boldsymbol{\pi}}_g = \begin{pmatrix} 1.6136 \times 10^{-5} \\ -0.0013 \\ -0.0046 \\ 0.0315 \\ -0.0417 \\ 0.0054 \\ 1.3544 \\ 0.0183 \\ -0.0036 \\ 0.0271 \\ -0.0129 \\ 3.4459 \end{pmatrix}, \quad \hat{\boldsymbol{\pi}}_{L,g} = \begin{pmatrix} 0.0016 \\ -0.0021 \\ -0.0093 \\ 0.3983 \\ -0.0409 \\ 0.0033 \\ 2.5458 \\ 0.005 \\ -0.0032 \\ 0.0629 \\ -0.0028 \\ 4.6775 \end{pmatrix}. \quad (42)$$

Considering the difference vectors $\boldsymbol{\varepsilon}_g(\boldsymbol{p}_{L,g})$ and $\hat{\boldsymbol{\varepsilon}}_g$ as in eqs. (21) and (25), we have for their symbolic non-zero components (i.e., for components 1, 2, 4, 7 and 12) and their associated estimates[1]

$$\boldsymbol{\varepsilon}_{g,nz}(\boldsymbol{p}_{L,g}) = \begin{pmatrix} c_{Ly}m_L \\ c_{Lx}m_L \\ c_{Lz}m_L \\ d_2 m_L \\ d_1 m_L \end{pmatrix} \Rightarrow \hat{\boldsymbol{\varepsilon}}_{g,nz} = \begin{pmatrix} 0.0016 \\ -8.13 \times 10^{-4} \\ 0.3667 \\ 1.1914 \\ 1.2316 \end{pmatrix}. \quad (43)$$

Using the reduced payload Jacobian $\boldsymbol{J}_{\boldsymbol{\varepsilon}_g,nz}$, we obtain the estimates

$$\hat{m}_L = 3.067\,\text{kg}, \qquad {}^7\hat{\boldsymbol{r}}_{7,cL} = \begin{pmatrix} -2.6 \cdot 10^{-4} \\ 5 \cdot 10^{-4} \\ 0.1196 \end{pmatrix}\,\text{m}. \quad (44)$$

These estimates are reasonably accurate. The remaining errors are attributed to noise in the joint torque measures, to neglecting static friction effects, as well as to simplifications made in establishing the ground-truth values in (39).

In order to estimate also the inertial parameters of the considered payload, one should handle a complete regressor, as in (11), which is rather cumbersome for a 7-dof robot as the KUKA LWR, needing high computational power to be evaluated symbolically. Therefore, to reduce the size of the regressor for inertial payload estimation, we designed

---

[1]As indicated in general by eq. (26), it is also possible for this robot to compute a numerical estimation $\hat{\boldsymbol{\varepsilon}}_g$ using the FRI function `GetCurrentGravityVector`, which returns the manufacturer's estimation of the gravity vector of the unloaded robot $\hat{\boldsymbol{g}}(\boldsymbol{q})$. Hence, we may avoid obtaining the two estimations of the coefficients $\hat{\boldsymbol{\pi}}_g$ and $\hat{\boldsymbol{\pi}}_{L,g}$, and use instead the joint torque measures retrieved statically with the loaded robot.
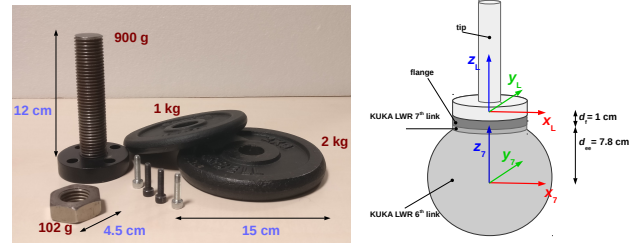

Fig. 4. The payload structure with variable weight used in the experiments.

simplified, but still sufficiently exciting trajectories to retrieve joint positions, velocities, accelerations and torque data to be used for identification. In particular, we designed a motion only for the first joint, keeping the other joints fixed in three different ways, but with the arm (links 2 to 7) always essentially straight and parallel to the ground:

- $\boldsymbol{q}_A(t) = \begin{pmatrix} q_1(t) & \frac{\pi}{2} & 0 & 0 & 0 & 0 & 0 \end{pmatrix}^T$
- $\boldsymbol{q}_B(t) = \begin{pmatrix} q_1(t) & \frac{\pi}{2} & 0 & 0 & 0 & -\frac{\pi}{2} & 0 \end{pmatrix}^T$
- $\boldsymbol{q}_C(t) = \begin{pmatrix} q_1(t) & \frac{\pi}{2} & 0 & 0 & -\frac{\pi}{2} & 0 & 0 \end{pmatrix}^T.$

With these configurations, motion of the first joint maximizes the dynamic effects of the inertial components of the payload, which is attached at the end of the arm. On the other hand, only a maximum of 19 dynamic coefficients are involved along these trajectories. For joint 1, $q_1(t)$ is a sinusoidal signal with increasing frequency, sweeping from low velocities and accelerations up to ± 100 deg/s and ± 150 deg/s^2, respectively. Each trajectory lasts for 15 seconds and is performed with and without the payload. Joint positions and torques are read every 5 ms and then off-line filtered using a low-pass Butterworth filter with a cutoff frequency 1 Hz. Joint velocities and accelerations are obtained by numerical differentiation from the filtered positions. Finally, 500 samples are extracted from the previous data sequences.

At this stage, one may compute the symbolic difference vector $\boldsymbol{\varepsilon}(\boldsymbol{p}_L)$ and its numerical estimate $\hat{\boldsymbol{\varepsilon}}$, as shown in eqs. (21) and (25). Again, this operation is performed at best by considering only the estimates $\hat{\boldsymbol{\varepsilon}}_{nz}$ of the non-zero symbolic elements $\boldsymbol{\varepsilon}_{nz}(\boldsymbol{p}_L)$. The payload Jacobian $\boldsymbol{J}_{\boldsymbol{\varepsilon},nz}$ can then be easily obtained from $\boldsymbol{\varepsilon}_{nz}(\boldsymbol{p}_L)$. However, in order to exploit all the information collected so far, we have stacked the two Jacobian matrices $\boldsymbol{J}_{\boldsymbol{\varepsilon}_g,nz}$ and $\boldsymbol{J}_{\boldsymbol{\varepsilon},nz}$ and the two numerical vector estimates $\hat{\boldsymbol{\varepsilon}}_{g,nz}$ (see eq. (43)) and $\hat{\boldsymbol{\varepsilon}}_{nz}$, producing a new complete estimate as

$$\hat{\boldsymbol{p}}_L = \begin{pmatrix} \boldsymbol{J}_{\boldsymbol{\varepsilon}_g} \\ \boldsymbol{J}_{\boldsymbol{\varepsilon}_\tau} \end{pmatrix}^{\#} \begin{pmatrix} \hat{\boldsymbol{\varepsilon}}_g \\ \hat{\boldsymbol{\varepsilon}}_\tau \end{pmatrix}. \quad (45)$$

We obtained the following numerical results:

$$\hat{m}_L = 3.041\,\text{kg}, \qquad {}^7\hat{\boldsymbol{r}}_{7,cL} = \begin{pmatrix} -7.5 \cdot 10^{-4} \\ -3.8 \cdot 10^{-3} \\ 0.1212 \end{pmatrix}\,\text{m},$$

$\hat{J}_{Lxx} = 0.157831, \ \hat{J}_{Lyy} = 0.044259, \ \hat{J}_{Lzz} = 0.003716,$

$\hat{J}_{Lxy} = 0.000795, \ \hat{J}_{Lxz} = -0.007835 \ \hat{J}_{Lyz} = -0.019714$

$$\text{kg} \cdot \text{m}^2. \quad (46)$$

TABLE I

NOMINAL AND ESTIMATED PARAMETERS FOR A LIGHT PAYLOAD

	m_L [kg]	r_{7,cL_x} [m]	r_{7,cL_y} [m]	r_{7,cL_z} [m]
Nominal value	0.144	0	0	0.1146
Estimated value	0.143	0.003	0.002	0.1124

These estimates have been successfully validated on different motion trajectories. Finally, we repeated the experiment using a very light payload. As reported in Tab. I, also in this case the mass and the position of the center of mass were estimated with high precision.

VI. MORE EXAMPLES AND USE OF PAYLOAD ESTIMATION

We consider two application examples involving the KUKA LWR 4+ arm, focusing for simplicity only on the estimation of non-inertial parameters of the payload, i.e., $\boldsymbol{p}_{L,g}$ in eq. (41), or, equivalently, assuming $\boldsymbol{J}_L = \boldsymbol{0}$ or that inertia is negligible.

A. Estimating with few data

In some industrial tasks, the robot needs to execute pick-and-move or pick-and-place operations, handling multiple objects with unknown/uncertain dynamic characteristics. Indeed, having a good and quick estimation of the dynamic parameters of the payload would allow a more accurate execution of the task, without wasting too much time. Ideally, for a reliable estimation of the payload a large number of data samples should be retrieved from different regions of the robot workspace. However, such a procedure is unpractical, both because of the amount of time needed and because of the restricted motions allowed in a typically cluttered workspace. With this in mind, we have evaluated the payload identification phase of our method when performing just a few small movements in the neighborhood of the Cartesian pick position. Only 10 samples are taken from static positioning of the robot with increments of $\pm 7°$ per joint around the pick configuration. When the robot moves to the next position in the list, it waits 1 sec before retrieving more reliable position and joint torque measurements. At the end, the payload mass and its CoM position are estimated as in Sec. V and the dynamic model is immediately updated[2]. We implemented a complete algorithm in C++ for such a pick-estimate-and-move operation, which can be seen in the accompanying video. For the nominal payload of about 3 kg in (39), we obtained the following estimates:

$$\hat{m}_L = 3.059 \text{ kg}, \qquad {}^7\hat{\boldsymbol{r}}_{7,cL} = \begin{pmatrix} -2.8 \cdot 10^{-3} \\ 1.1 \cdot 10^{-2} \\ 0.1283 \end{pmatrix} \text{ m}. \quad (47)$$

Despite the estimation errors have slightly increased, the results are still satisfactory. This can be appreciated also from the torque comparison on a validation trajectory shown in Fig. 5: torque estimation errors remain always below $1.5 \div 3$ Nm as a maximum.

[2]Using a commercial PC with an i7 Intel processor and 16 GB of RAM memory, all computations take less than 1 second.
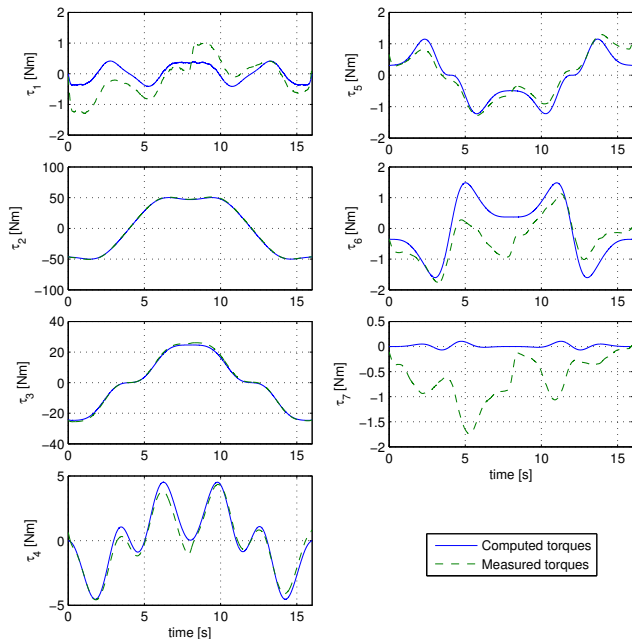

Fig. 5. Comparison of measured torques $\boldsymbol{\tau}_J$ [dashed-green] and computed torques $\hat{\boldsymbol{\tau}}_J$ [solid-blue] in a validation test on the KUKA LWR robot carrying the medium-weight payload (39). The computed torques use the estimated values in (47).

B. Sensorless collision detection

In recent years, much attention has been devoted to collision detection strategies able to ensure safer human-robot interaction. One of the most successful strategies [2], which was also implemented by KUKA in their lightweight robot series (LWR and iiwa), is based on monitoring a so-called *residual vector* $\boldsymbol{r}(t) \in \mathbb{R}^n$, which is computed online on the basis of a previously identified dynamic model of the robot. The residual remains nominally at zero during free robot motion. When one or more components of $\boldsymbol{r}(t)$ exceed some predefined threshold, a collision is detected and the robot can react, e.g., by stopping. The residual returns exponentially to zero as soon as there is no contact anymore, so that the robot can restart its motion task. Indeed, all these nice properties are corrupted by the addition of an unknown payload, which changes the robot dynamic model and thus drives away from zero also an untuned residual. This would generate false positives, i.e., a contact is detected when there is none, or false negatives, disregarding a contact because of the large threshold used to overcome model uncertainties.

To overcome these critical issues, the proposed payload estimation method can be integrated directly in the evaluation of an estimated residual $\hat{\boldsymbol{r}}(t)$ as

$$\hat{\boldsymbol{r}} = \boldsymbol{K}_I \left(\hat{\boldsymbol{M}}(\boldsymbol{q})\dot{\boldsymbol{q}} - \int_0^t \left(\boldsymbol{\tau}_J + \hat{\boldsymbol{S}}^T(\boldsymbol{q}, \dot{\boldsymbol{q}})\dot{\boldsymbol{q}} - \hat{\boldsymbol{g}}^L(\boldsymbol{q}) + \hat{\boldsymbol{r}} \right) ds \right), \quad (48)$$

where $\boldsymbol{K}_I > 0$ is a diagonal gain matrix, $\boldsymbol{\tau}_J$ is measured, the estimates of $\boldsymbol{M}$ and $\boldsymbol{S}$ are obtained without payload, while only $\hat{\boldsymbol{g}}^L$ uses the $\hat{\boldsymbol{p}}_{L,g}$ estimated as in Sec. VI-A. The accompanying video shows two experiments with multiple
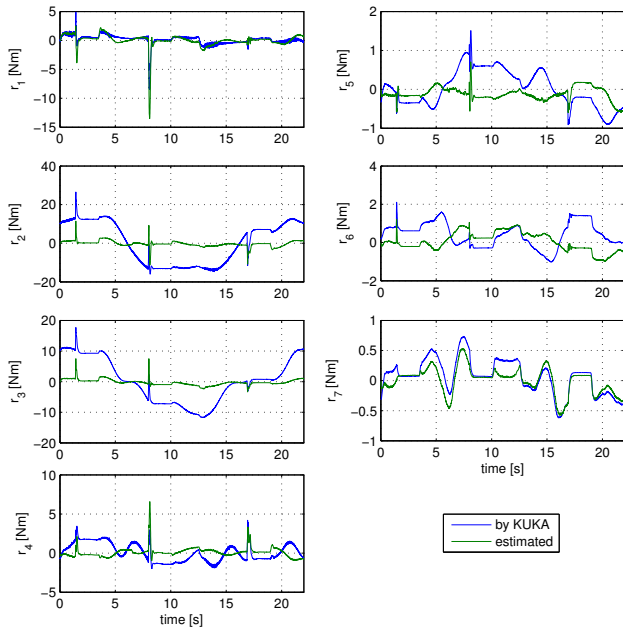
Fig. 6. Monitoring three human-robot collisions (at $t = 1$, 8, and 17 sec) during robot motion: signals from KUKA FRI [blue] and residuals computed with our eq. (48), using the estimated mass and position of the payload [green]. All three collisions are detected by our residual, when at least one components exceeds a threshold of 6 Nm. Conversely, collisions are hardly detectable by the KUKA FRI since its signals often exceed this threshold during free motion.

human-robot contacts detected by using (48) with a threshold of 6 Nm. At every detected collision, the robot stops for 2 sec and then resumes motion. Figure 6 illustrates the improvement when using a tuned residual instead of the embedded external torque detector of the KUKA FRI.

VII. CONCLUSIONS

We have revisited the problem of estimating the dynamic parameters of an unknown payload held by the robot end effector, using a method that relies on the identification of the robot dynamic coefficients without and with the payload, We have exploited the linear changes that occur in the symbolic expressions of the original dynamic coefficients when a payload is added. The method was presented here as a two-stage identification procedure, but estimation of payload parameters can be implemented also in a single stage, combining data collected both from loaded and unloaded experiments. With respect to the state-of-the-art [15], we have clarified once for all that the approach does not require the use of any particular kinematic frame convention. Moreover, it can be tailored to the estimation of only a subset of payload dynamic parameters, and is accurate enough to handle also very light payloads or few small motions in the data collection for identification. It can also be simplified when the robot control software already provides a routine that computes the expected joint torques without payload on the current (loaded) motion, so that there is no need to perform experiments without the payload. The results obtained in various case studies provide evidence

of a reliable and consistent performance. The estimated payload parameters can be used in a recursive Newton-Euler implementation of model-based control algorithms, together with a set of physically feasible dynamic parameters that are extracted from the previously identified dynamic coefficients of the unloaded robot. Finally, as an important application in physical human-robot interaction, we have shown the dramatic improvement that payload estimation can have on the model-based collision detection and isolation method of [2], which is the most efficient one available at present.

REFERENCES

[1] B. Siciliano, L. Sciavicco, L. Villani, and G. Oriolo, *Robotics: Modeling, Planning and Control*, 3rd ed. London: Springer, 2008.

[2] A. De Luca, A. Albu-Schäffer, S. Haddadin, and G. Hirzinger, "Collision detection and safe reaction with the DLR-III lightweight robot arm," in *Proc. IEEE/RSJ Int. Conf. on Intelligent Robots and Systems*, 2006, pp. 1623–1630.

[3] E. Magrini, F. Flacco, and A. De Luca, "Control of generalized contact motion and force in physical human-robot interaction," in *Proc. IEEE Int. Conf. on Robotics and Automation*, 2015, pp. 2298–2304.

[4] E. Magrini and A. De Luca, "Hybrid force/velocity control for physical human-robot collaboration tasks," in *Proc. IEEE/RSJ Int. Conf. on Intelligent Robots and Systems*, Oct. 2016.

[5] J. Hollerbach, W. Khalil, and M. Gautier, "Model identification," in *Handbook of Robotics*, B. Siciliano and O. Khatib, Eds. Springer, 2008, pp. 321–344.

[6] W. Khalil and E. Dombre, *Modeling, Identification and Control of Robots*. Hermes Penton London, 2002.

[7] J. Swevers, W. Verdonck, and J. De Schutter, "Dynamic model identification for industrial robots," *IEEE Control Systems Mag.*, vol. 27, no. 5, pp. 58–71, 2007.

[8] C. Gaz, F. Flacco, and A. De Luca, "Identifying the dynamic model used by the KUKA LWR: A reverse engineering approach," in *Proc. IEEE Int. Conf. on Robotics and Automation*, 2014, pp. 1386–1392.

[9] A. Jubien, M. Gautier, and A. Janot, "Dynamic identification of the Kuka LightWeight Robot: Comparison between actual and confidential Kuka's parameters," in *Proc. IEEE/ASME Int. Conf. on Advanced Intelligent Mechatronics*, 2014, pp. 483–488.

[10] Coppelia Robotics, "V-REP virtual robot experimentation platform." [Online]. Available: http://www.coppeliarobotics.com

[11] R. Featherstone, *Robot Dynamics Algorithms*. Kluwer, 1987.

[12] C. Gaz, F. Flacco, and A. De Luca, "Extracting feasible robot parameters from dynamic coefficients using nonlinear optimization methods," in *Proc. IEEE Int. Conf. on Robotics and Automation*, 2016, pp. 2075–2081.

[13] C. G. Atkeson, C. H. An, and J. M. Hollerbach, "Estimation of inertial parameters of manipulator loads and links," *The International Journal of Robotics Research*, vol. 5, no. 3, pp. 101–119, 1986.

[14] H. Kawasaki and K. Nishimura, "Terminal-link parameter estimation of robotic manipulators," *IEEE Journal on Robotics and Automation*, vol. 4, no. 5, pp. 485–490, Oct 1988.

[15] W. Khalil, M. Gautier, and P. Lemoine, "Identification of the payload inertial parameters of industrial manipulators," in *Proc. IEEE Int. Conf. on Robotics and Automation*, 2007, pp. 4943–4948.

[16] M. B. Leahy, M. A. Johnson, and S. K. Rogers, "Neural network payload estimation for adaptive robot control," *IEEE Trans. on Neural Networks*, vol. 2, no. 1, pp. 93–100, Jan 1991.

[17] Z. Shareef, F. Reinhart, and J. Steil, "Generalizing a learned inverse dynamic model of KUKA LWR IV+ for load variations using regression in the model space," in *2016 IEEE/RSJ International Conference on Intelligent Robots and Systems (IROS)*, Oct 2016, pp. 606–611.

[18] W. Rackl, R. Lampariello, and G. Hirzinger, "Robot excitation trajectories for dynamic parameter estimation using optimized B-splines," in *IEEE International Conference on Robotics and Automation (ICRA)*, May 2012, pp. 2042–2047.

[19] *KUKA Controller KR C2 lr Specification*, KUKA Laboratories GmbH, D-86165 Augsburg, Germany, 2012, version V5 en, pages 14–15.

[20] *KUKA.FastResearchInterface 1.0*, KUKA System Technology (KST), D-86165 Augsburg, Germany, 2011, version 2.